Construction of a plasminogen activator inhibitor-1 variant without measurable affinity to vitronectin but otherwise normal

Jan K. Jensen*, Michelle K.V. Durand, Sune Skeldal, Daniel M. Dupont, Julie S. Bødker, Troels Wind, Peter A. Andreasen

Laboratory of Cellular Protein Science, Department of Molecular Biology, Aarhus University, Gustav Wieds Vej 10C, 8000 C Aarhus, Denmark

Received 2 September 2003; revised 3 November 2003; accepted 11 November 2003

First published online 8 December 2003

Edited by Gianni Cesareni

Abstract Vitronectin (VN) and plasminogen activator inhibitor-1 (PAI-1) have important functional interactions: VN stabilises the protease inhibitory activity of PAI-1 and PAI-1 inhibits binding of adhesion receptors to VN. Having previously mapped the PAI-1 binding area for VN, we have now constructed a PAI-1 variant, R103A-M112A-Q125A, without measurable affinity to VN, but with full protease inhibitory activity and endocytosis receptor binding. As a tool for evaluating the physiological and pathophysiological functions of the PAI-1–VN interaction, our new variant is far superior to the previously widely used PAI-1 variant Q125K, which we have found possesses an only about 10-fold reduced affinity to VN.

Key words: Plasminogen activator inhibitor-1; Plasminogen; Serpin; Vitronectin; Adhesion

1. Introduction

Plasminogen activator inhibitor-1 (PAI-1) is a mammalian $M_r \sim 50\,000$ extracellular protein. Mice with a disrupted *PAI-1* gene grow to adulthood and are fertile, but display a mild hyperfibrinolytic phenotype with a decreased tendency to thrombosis (for a review, see [1]). Accordingly, PAI-1 is a fast and specific inhibitor of the serine protease tissue-type plasminogen activator, a key fibrinolytic enzyme. PAI-1 is also a fast and specific inhibitor of the serine protease urokinase-type plasminogen activator (uPA), which is implicated in physiological and pathophysiological tissue remodelling (for a review, see [2]).

PAI-1 belongs to the serpin class of protease inhibitors. The serpin inhibitory mechanism begins with the protease attacking the P_1–P_1' bond in the serpin reactive centre loop (RCL), but at the enzyme–acyl intermediate stage, the N-terminal part of the RCL inserts into a central β-sheet A, pulls the protease to the opposite pole of the serpin, distorts it, and halts its completion of the catalytic cycle. The energy needed for protease distortion stems from stabilisation of the serpin in the 'relaxed' conformation with the inserted RCL, as compared to the 'stressed', unstable active conformation with the surface-exposed RCL (for reviews, see [1,3]). PAI-1 can also assume the inactive, relaxed, so-called latent state in which the intact RCL is inserted into β-sheet A [4]. During RCL insertion, the flexible joint region (α-helices E and F, β-strands 1A and 2A, residues 95–145) lateral to the β-sheet A also changes conformation (for a review, see [1]).

Some of the biological functions of PAI-1 seem to be related to interactions with molecules other than plasminogen activators. First, stressed, but not relaxed, PAI-1 binds with high affinity to the $M_r \sim 75\,000$ extracellular matrix and blood plasma glycoprotein vitronectin (VN) and is thereby protected against latency transition (for a review, see [1]) and inactivation by organo-chemical ligands, including 4,4′-dianilino-1,1′-bisnaphthyl-5,5′-disulfonic acid (bis-ANS) [5,6]. Moreover, active PAI-1 acts anti-adhesively by competing with integrins and the uPA receptor (uPAR) for binding to VN (for a review, see [1]). Second, complexes of plasminogen activators and PAI-1 bind to endocytosis receptors of the low-density lipoprotein receptor family including LRP. This binding is a mechanism for clearing the complexes from the extracellular space, but may also activate intracellular signaling pathways (for a review, see [7]). PAI-1 variants specifically inactivated with respect to each of the specific molecular interactions are needed in order to sort out the biological functions of each interaction.

VN binds to the flexible joint region of PAI-1. In the pioneering work by Lawrence et al. [8], screening of PAI-1 variants produced by random mutagenesis was used to show that the substitutions L118P and Q125K resulted in reduced VN binding. A later report suggested implication of residues 116–120 in VN binding [9]. Investigations with the less accurate methods of antibody competition [10] and PAI-1–PAI-2 chimeras [11] also pointed towards the flexible joint region of PAI-1. Using a novel strategy, based on identification of amino acid (aa) residues necessary for VN protection of PAI-1 against inactivation by bis-ANS, we defined 10 aa residues forming a VN binding surface in the flexible joint region [12]. The subsequently published X-ray crystal structure analysis of the complex between PAI-1 and the N-terminal 44 aa somatomedin B domain of VN [13] was in full agreement with these results. We have now constructed a PAI-1 variant without measurable affinity to VN, but with full ability to inhibit

*Corresponding author.
E-mail address: jkj@mb.au.dk (J.K. Jensen).

Abbreviations: aa, amino acid; bis-ANS, 4,4′-dianilino-1,1′-bisnaphthyl-5,5′-disulfonic acid; DFP, diisopropyl fluorophosphate; FBS, foetal bovine serum; LRP, low-density lipoprotein receptor-related protein; Mab-2, monoclonal anti-PAI-1 antibody clone 2; PAI-1, plasminogen activator inhibitor-1; PBS, phosphate-buffered saline; PMA, phorbol 12-myristate 13-acetate; RU, response units; SPR, surface plasmon resonance; uPA, urokinase plasminogen activator; uPAR, uPA receptor; VN, vitronectin; wt, wild-type

0014-5793/03/$30.00
doi:10.1016/S0014-5793(03)01405-4

plasminogen activators and to interact with endocytosis receptors.

2. Materials and methods

2.1. Materials

PAI-1 wild type (wt) and mutants were expressed by and purified from *Escherichia coli* [12] or human HEK293T cells [14]. The PAI-1 aa numbering system used was based on the determination of the N-terminal sequence of the protein as S1-A2-V3-H4-H5... [15]. Human multimeric VN was from BD Biosciences (Franklin Lakes, NJ, USA). Human uPA was from Wakamoto Pharmaceuticals (Tokyo, Japan). uPA was inactivated with diisopropyl fluorophosphate (DFP) [16]. uPAR C-terminally truncated after D277 (soluble uPAR) was a kind gift from Gunilla Høyer-Hansen, Finsen Laboratory [17]. Mab-2 is a previously described monoclonal antibody against PAI-1 [18–20]. Bis-ANS was from Molecular Probes (Eugene, OR, USA). RPMI 1640 cell culture medium and foetal bovine serum (FBS) were from Cambrex, BioWhittaker Europe (Belgium). S-2444 (pyro-Glu-Gly-Arg-*p*-nitroanilide) was from Chromogenix (Mölndal, Sweden). Phorbol 12-myristate 13-acetate (PMA) was from Sigma (St. Louis, MO, USA).

2.2. PAI-1 activity measurements

The specific inhibitory activities of PAI-1 wt and mutants were measured as before [12]. To determine the IC_{50} values for bis-ANS neutralisation of PAI-1, the specific inhibitory activities of PAI-1, without VN or preincubated with VN at concentrations of about 20 μM, were determined in the presence of several concentrations of bis-ANS. The IC_{50} values were determined as the bis-ANS concentration halving the specific inhibitory activity [12]. To measure the rate of latency transition, samples were withdrawn from solutions with 450 nM PAI-1, with or without 450 nM VN, for measurement of specific inhibitory activity after different time periods of incubation at 37°C. The latency transition half-lives were calculated from semi-logarithmic plots of specific inhibitory activity versus time. To evaluate Mab-2 neutralisation of PAI-1, the specific inhibitory activity of PAI-1, without VN or preincubated with VN at concentrations of about 20 μM, was measured at different Mab-2 concentrations. Second-order rate constants were determined as described [21].

2.3. Binding of uPA–PAI-1 complex to LRP

The binding of [^{125}I]uPA–PAI-1 complex to LRP immobilised on the solid phase of microtitre plates was measured as described [16], using PAI-1 wt and mutants expressed by HEK293T cells [14], and a [^{125}I]uPA–PAI-1 complex concentration of 20 pM.

2.4. Solid-phase VN–PAI-1 binding assay

VN was coated onto the solid phase of Maxisorb microtitre plates (Nunc, Roskilde, Denmark), using 100 μl 0.5 μg/ml VN in 50 mM $NaHCO_3$, pH 9.6, per well and incubation overnight at 4°C. The wells were blocked with 2% skim milk powder in phosphate-buffered saline (PBS). Aliquots of 100 μl of PBS were added to the wells, with PAI-1 in concentrations between 250 nM and 3 pM, followed by 1 h incubation at room temperature. The relative amounts of PAI-1 bound to the solid phase were estimated with a layer of rabbit polyclonal anti-PAI-1 antibodies, a layer of peroxidase-conjugated swine anti-rabbit IgG, and a peroxidase reaction. The VN affinity of the respective PAI-1 variants relative to that of PAI-1 wt was calculated as the ratios between the concentrations of variant and wt giving the same signal.

2.5. Binding analysis by surface plasmon resonance (SPR)

All analyses were performed with a BIACORE X™ instrument, using a CM5™ chip blocked with ethanolamine as reference in flow cell 2. To analyse the binding of PAI-1 variants to VN, a CM5™ chip was coated with 50 nM VN in 10 mM Na-acetate, pH 5.0, by a standard amine coupling protocol until a density of approximately 2400 response units (RU) or approximately 33 fmol was accumulated on the chip. Eighty μl of PAI-1 wt or variants were injected in concentrations of 7, 10 and 14 nM at a flow rate of 20 μl/min. To elute the remaining PAI-1 after each round of injection, 10 mM glycine-HCl, pH 2.0 was injected until the baseline level was reached again. K_d values were estimated from the association and dissociation rates, using the software provided with the BIACORE X™ instrument, assuming 1:1 stoichiometry.

To analyse the uPAR–VN binding, a CM5™ chip was coated with soluble uPAR (0.5 μM in 10 mM Na-acetate, pH 4.5) by a standard amine coupling protocol until approximately 2300 RU or approximately 40 fmol were accumulated on the chip. The immobilised uPAR was kept saturated with DFP-inactivated uPA by constantly using a running buffer (10 mM HEPES, 140 mM NaCl, 3 mM EDTA, pH 7.4) supplemented with 12 pM DFP-inactivated uPA and by injecting 50 μl 100 nM DFP-inactivated uPA before each experiment. For each experiment, VN was injected to saturation of the immobilised uPAR (50 μl 200 nM VN, corresponding to approximately 500 RU being immobilised), followed by running buffer for 400 s. Fifty μl of PAI-1 wt or mutants, in the concentration range of 1–200 nM, were then injected, and the SPR signal from the chip followed for 280 s. Between experiments, any VN remaining on the chip was eluted with 50 μl 200 nM PAI-1 wt. A flow rate of 10 μl/min was used throughout.

2.6. Binding of U937 cells to VN

[^{125}I]VN was prepared as previously described [22]. U937 cells were cultured in RPMI 1640 with 10% FBS. Cells (10^6/ml) were incubated with PMA (160 nM) for 20 h. Adherent cells were scraped off the disc with a rubber policeman. The cells were washed with RPMI 1640 supplemented with 0.02% bovine serum albumin. [^{125}I]VN was incubated for 90 min on ice with or without PAI-1 additions as indicated for each experiment, followed by incubation with 1×10^5 cells/ml on ice for 90 min with a final [^{125}I]VN concentration of 10 pM. Cells were washed and harvested by centrifugation in a microfuge (12 000 rpm, 3.5 min) in the presence of 20% sucrose and the amount of cell-associated [^{125}I]VN in the pellet quantified in a γ counter. The amounts of bound [^{125}I]VN were corrected for non-specific binding, i.e. the binding with 10 pM [^{125}I]VN plus 10 nM non-radioactive VN.

3. Results and discussion

To localise the VN binding area of PAI-1, we previously constructed about 40 variants of PAI-1 with alanine substitutions in the flexible joint region. Many of these had a reduced specific inhibitory activity, due to an increased tendency to substrate behaviour or an increased fraction of the PAI-1 molecules being in a latent state. A direct VN–PAI-1 binding assay would therefore give misleading results, as any relaxed form of PAI-1 has a low affinity to VN. We therefore chose an alternative approach, measuring the interaction of VN with only the fraction of active PAI-1 in the preparations. VN protects PAI-1 wt against bis-ANS inactivation, and we were able to show that alanine substitutions of F100, R103, M112, K124, Q125, I137, D140, and W141 led to an only partial protection against bis-ANS [12] (Table 1), strongly suggesting that these residues form a VN binding surface on PAI-1.

However, some of the variants in fact had a specific inhibitory activity and a latency transition rate that were indistinguishable from those of PAI-1 wt. This was true for, among others, PAI-1 R103A, PAI-1 M112A, and PAI-1 Q125A. In order to obtain a variant with a complete lack of VN affinity, but otherwise normal, we combined these three substitutions into one molecule. The triple substitution R103A-M112A-Q125A led to a PAI-1 variant that did not differ significantly from PAI-1 wt with respect to specific inhibitory activity (Table 1), latency transition rate (Table 1), second-order rate constant for the uPA–PAI-1 reaction (data not shown), or binding of uPA–PAI-1-complex to LRP (Fig. 1). But the triple mutant completely lacked the ability to be protected against bis-ANS by VN (Table 1) and it had a more than 3000-fold reduced affinity for VN as compared to the PAI-1 wt in an ELISA-type binding assay (Table 1). In contrast, introduction of each mutation individually into PAI-1 led to

Table 1
Functional properties of PAI-1 variants

PAI-1 variant	bis-ANS susceptibility		Specific inhibitory activity (percent of theoretical maximum)	Latency transition half-life (min)		VN binding (fold reduced binding, in solid phase binding assay)
	IC_{50} without VN (μM)	IC_{50} with VN (μM)		Without VN	With VN	
wt	0.73 ± 0.06 (3)	51 ± 18 (6)[a]	83 ± 11 (14)	67 ± 3 (15)	118 ± 26 (4)[b]	1.0
R103A	0.63 ± 0.15 (3)	4.9 ± 2.5 (3)[a]	108 ± 9 (3)	63 ± 4 (3)	102 ± 3 (3)[b]	4.6 ± 1.2 (4)[c]
M112A	0.73 ± 0.23 (3)	5.3 ± 1.7 (3)[a]	92 ± 24 (3)	66 ± 2 (3)	107 ± 4 (3)[b]	1.3 ± 0.4 (3)
Q125A	0.63 ± 0.10 (4)	4.8 ± 3.2 (4)[a]	81 ± 5 (3)	43 ± 2 (3)	85 ± 5 (3)[b]	1.0 ± 0.0 (3)
Q125K	0.68 ± 0.11 (3)	2.4 ± 1.0 (3)[a]	77 ± 3 (3)	58 ± 9 (3)	110 ± 6 (3)[b]	2.8 ± 1.1 (3)
R103A-M112A-Q125A	0.70 ± 0.10 (3)	0.68 ± 0.06 (3)	79 ± 11 (3)	59 ± 3 (3)	45 ± 4 (3)	> 3000 (3)[c]

IC_{50} for neutralisation by bis-ANS in the absence or presence of VN, specific inhibitory activity, latency transition half-life, and fold reduced binding to VN of the indicated PAI-1 variants were measured as described in Section 2. The table shows means, S.D., and numbers of determinations.
[a]Significantly different from IC_{50} without VN ($P < 0.05$).
[b]Significantly larger than half-life without VN ($P < 0.005$).
[c]Significantly different from 1 ($P < 0.01$).

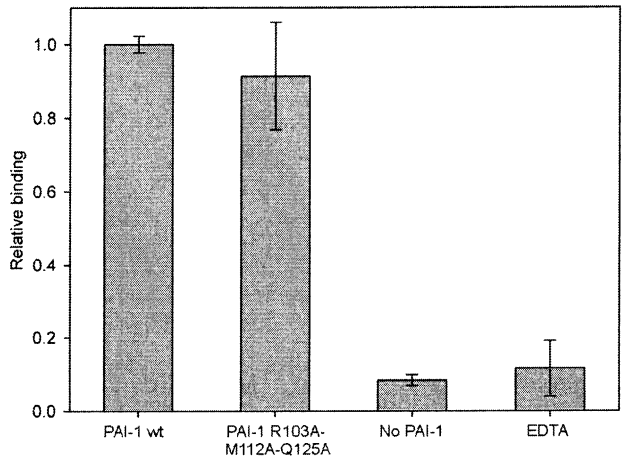

Fig. 1. Analysis of binding of uPA–PAI-1 complex to LRP. Binding of the indicated PAI-1 variants, expressed in HEK293T cells, in complex with [^{125}I]uPA to immobilised LRP was measured in a solid-phase assay. Incubations without PAI-1 or in the presence of 10 mM EDTA were included as controls. The concentrations of [^{125}I]uPA–PAI-1 complex or [^{125}I]uPA were 20 pM. The binding is expressed relative to that of [^{125}I]uPA in complex with PAI-1 wt.

an only slightly reduced VN binding, and a PAI-1 variant widely used as a non-VN binder, Q125K [8], had an only about three-fold reduced binding to VN in this assay (Table 1). In addition, we used SPR analysis to determine the K_d values for the binding of PAI-1 wt and PAI-1 Q125K to immobilised VN. We found values of 0.22 ± 0.2 nM ($n = 4$) and 2.8 ± 1.4 nM ($n = 5$) for PAI-1 wt and PAI-1 Q125K, respectively. Thus, PAI-1 Q125K has an at least 10-fold reduced affinity compared to PAI-1 wt in this assay. The K_d value for PAI-1 R103A-M112A-Q125A could not be determined in this assay as only unspecific binding to the VN-coated chip was detected (Fig. 2).

We next characterised the triple mutant and PAI-1 Q125K with respect to a number of previously observed PAI-1–VN interactions. First, VN delayed the latency transition of PAI-1

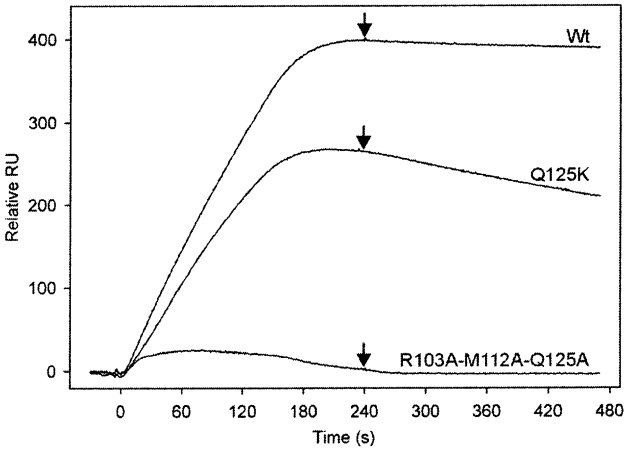

Fig. 2. Analysis of binding of PAI-1 variants to VN by SPR. Approximately 33 fmol of VN was coupled to a CM5™ BIACORE chip. At time zero, 14 nM of the indicated PAI-1 variants, expressed in *E. coli*, were applied to the chip for 240 s. The time point for end of injection is indicated by black arrows. Each of the experiments shown is a typical one out of a total of three. Note that the signal for PAI-1 R103A-M112A-Q125A declines before the injections stops.

Q125K in a manner indistinguishable from that of PAI-1 wt, while the latency transition of the triple mutant was not affected by VN (Table 1). Second, we previously demonstrated that VN potentiates the inactivation of PAI-1 by the monoclonal antibody Mab-2. In the absence of VN, Mab-2 is a weak inactivator of PAI-1 while in the presence of VN, PAI-1 is inactivated by nM concentrations of Mab-2 [19,20]. The susceptibility of PAI-1 Q125K to Mab-2 was identical to that of PAI-1 wt in the absence and presence of VN, but the susceptibility of the triple mutant to Mab-2 was completely unaffected by VN (Fig. 3). Third, we measured the ability of the PAI-1 variants to compete with uPAR for binding to VN by SPR analysis. uPAR was immobilised covalently on a BIACORE™ chip, and a complex between uPAR, DFP-inactivated uPA, and VN assembled on the chip. uPA increases the affinity of uPAR to VN (for a review, see [1]). DFP-inactivated uPA was used to avoid uPA–PAI-1 interaction. Exposure of the uPAR–uPA–VN complex to PAI-1 wt led to dissociation of VN from the complex, with a rate increasing in the PAI-1 concentration range of 5–50 nM. PAI-1 Q125K also caused dissociation of VN, although about five-fold higher concentrations were needed to achieve the same dissociation rate as with PAI-1 wt. In contrast, 200 nM PAI-1 R103A-M112A-Q125A did not cause measurable dissociation of VN from the complex (Fig. 4). PAI-1 did not interfere with the binding of DFP-inactivated uPA to uPAR on the chip (data not shown).

Furthermore, we measured the ability of the PAI-1 variants to inhibit the binding of U937 cells to VN, which is mediated by uPAR [23]. The binding of [^{125}I]VN to U937 cells could be totally inhibited by sufficiently high concentrations of PAI-1 wt or PAI-1 Q125K. The concentrations causing half maximal inhibition was very close to the K_d values determined by SPR analysis. In contrast, PAI-1 R103A-M112A-Q125A did not measurably inhibit the binding in concentrations up to 30 nM (Fig. 5).

In conclusion, we have constructed a triple mutant of PAI-1 without measurable affinity to VN, but indistinguishable from PAI-1 wt with respect to the interaction with plasminogen activators and LRP. In assays testing several different functional consequences of the PAI-1–VN binding, the triple mutant did not respond measurably to VN. In contrast, while Q125K did have a significantly reduced affinity to VN, the reduction was not large enough to render it unresponsive to VN in all respects. In fact, in assays with the highest PAI-1 concentrations, it was indistinguishable from wt. The new

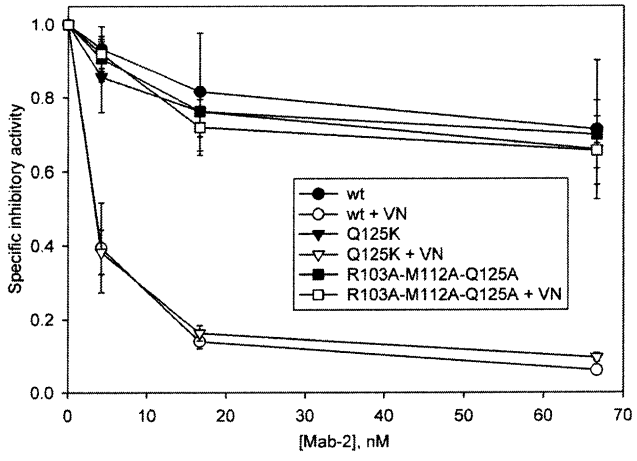

Fig. 3. Effect of VN on inactivation of PAI-1 by Mab-2. The figure shows the specific inhibitory activities, relative to that of control, of the indicated combinations of PAI-1 variants and VN, at the indicated concentrations of Mab-2. All PAI-1 variants were expressed in *E. coli*. Means and S.D. of triple determinations are indicated.

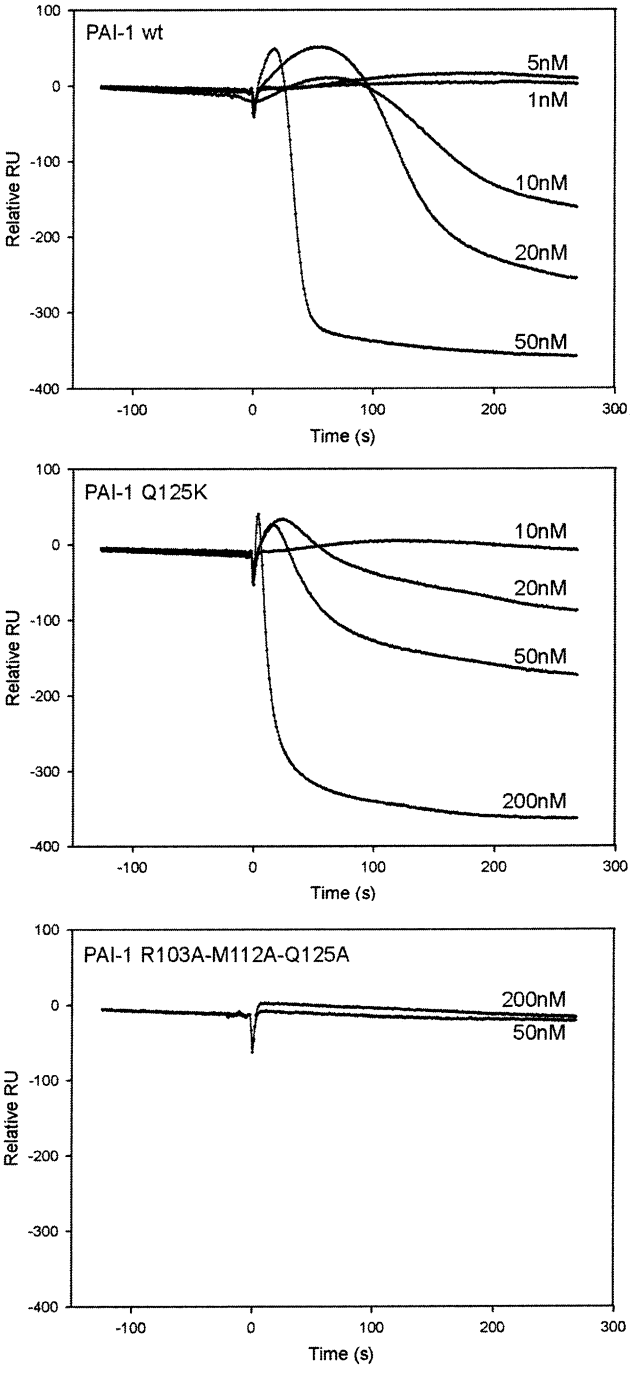

Fig. 4. Analysis of PAI-1 competition with uPAR for VN binding by SPR. Approximately 40 fmol of soluble uPAR was coupled to a CM5™ BIACORE chip. The immobilised uPAR was saturated with DFP-inactivated uPA and VN. At time zero, the indicated concentrations of the indicated PAI-1 variants, expressed in *E. coli*, were applied to the chip. The initial increase in material bound to the chip after application of PAI-1 presumably occurs because some of the units of the multimeric VN on the chip are not engaged with uPAR and thus free to bind PAI-1. Each of the experiments shown is a typical one out of a total of three.

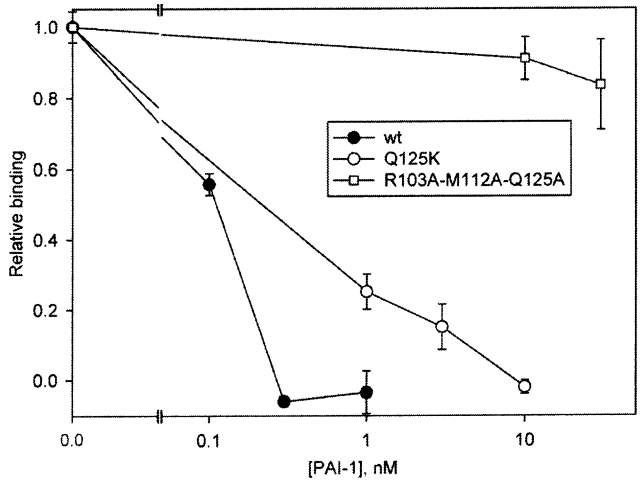

Fig. 5. PAI-1 inhibition of uPAR-mediated VN binding to U937 cells. The figure shows the relative binding of 10 pM [^{125}I]VN to U937 cells in the presence of the indicated PAI-1 variants, expressed in *E. coli*, in the indicated concentrations. Means and S.D. of triple determinations are indicated.

variant therefore represents an important and reliable tool for evaluating molecular aspects as well as physiological and pathophysiological functions of the PAI-1–VN interaction.

Acknowledgements: This work was supported by grants from the Danish Cancer Society, the Carlsberg Foundation, the Danish Natural Science Research Council, the NOVO Nordisk Foundation, and the Danish Research Agency. J.K.J. is the recipient of a Ph.D. fellowship from the *i*NANO School, Aarhus University.

References

[1] Wind, T., Hansen, M., Jensen, J.K. and Andreasen, P.A. (2002) Biol. Chem. 283, 21–36.
[2] Andreasen, P.A., Kjøller, L., Christensen, L. and Duffy, M.J. (1997) Int. J. Cancer 72, 1–22.
[3] Ye, S. and Goldsmith, E.J. (2001) Curr. Opin. Struct. Biol. 11, 740–745.
[4] Mottonen, J., Strand, A., Symersky, J., Sweet, R.M., Danley, D.E., Geoghegan, K.F., Gerard, R.D. and Goldsmith, E.J. (1992) Nature 355, 270–273.
[5] Egelund, R., Einholm, A.P., Pedersen, K.E., Nielsen, R.W., Christensen, A., Deinum, J. and Andreasen, P.A. (2001) J. Biol. Chem. 276, 13077–13086.
[6] Jensen, S., Kirkegaard, T., Pedersen, K.E., Busse, M., Preissner, K.T., Rodenburg, K.W. and Andreasen, P.A. (2002) Biochim. Biophys. Acta 1597, 301–310.
[7] Nykjær, A. and Willnow, T.E. (2002) Trends Cell Biol. 12, 273–280.
[8] Lawrence, D.A., Berkenpas, M.B., Palaniappan, S. and Ginsburg, D. (1994) J. Biol. Chem. 269, 15223–15228.
[9] Arroyo de Prada, N.A., Schroeck, F., Schmidt, E.-K., Muehlenweg, B., Twellmeyer, J., Sperl, S., Wilhelm, O.G., Schmitt, M. and Magdolen, V. (2002) Eur. J. Biochem. 269, 184–192.
[10] van Meijer, M., Gebbink, R.K., Preissner, K.T. and Pannekoek, H. (1994) FEBS Lett. 352, 342–346.
[11] Padmanabhan, J. and Sane, D.C. (1995) Thromb. Haemost. 73, 829–834.
[12] Jensen, J.K., Wind, T. and Andreasen, P.A. (2002) FEBS Lett. 521, 91–94.
[13] Zhou, A., Huntington, J.A., Pannu, N.S., Carell, R.W. and Read, R.J. (2003) Nat. Struct. Biol. 10, 541–544.
[14] Hansen, M., Busse, M.N. and Andreasen, P.A. (2001) Eur. J. Biochem. 268, 6274–6283.
[15] Andreasen, P.A., Riccio, A., Welinder, K.G., Douglas, R., Sartorio, R., Nielsen, L.S., Oppenheimer, C., Blasi, F. and Danø, K. (1986) FEBS Lett. 209, 213–218.
[16] Nykjær, A., Kjøller, L., Cohen, R.L., Lawrence, D.A., Garni-Wagner, B.A., Todd, R.F., van Zonneveld, A.J., Gliemann, J. and Andreasen, P.A. (1994) J. Biol. Chem. 269, 25668–25676.
[17] Ploug, M., Kjalke, M., Rønne, E., Weidle, U., Høyer-Hansen, G. and Danø, K. (1993) J. Biol. Chem. 268, 17539–17546.
[18] Nielsen, L.S., Andreasen, P.A., Grøndahl-Hansen, J., Huang, J.-Y., Kristensen, P. and Danø, K. (1986) Thromb. Haemost. 55, 206–212.
[19] Schousboe, S.L., Egelund, R., Kirkegaard, T., Preissner, K.T., Rodenburg, K.W. and Andreasen, P.A. (2000) Thromb. Haemost. 83, 742–751.
[20] Wind, T., Jensen, M.A. and Andreasen, P.A. (2001) Eur. J. Biochem. 268, 1095–1106.
[21] Petersen, H.H., Hansen, M., Schousboe, S.L. and Andreasen, P.A. (2001) Eur. J. Biochem. 268, 4430–4439.
[22] Nykjær, A., Kjøller, L., Cohen, R.L., Lawrence, D.A., Carni-Wagner, B.A., Todd, R.F., van Zonneveld, A.J., Gliemann, J. and Andreasen, P.A. (1994) J. Biol. Chem. 269, 25668–25676.
[23] Deng, G., Curriden, S.A., Wang, S., Rosenberg, S. and Loskutoff, D.J. (1996) J. Cell Biol. 134, 1563–1571.